interstitial mechanism in the high-pressure range and a vacancy mechanism only in the low-pressure range where a "fine-structure" search is lacking in Ref. 21.

ACKNOWLEDGMENT

The authors would like to thank L. Filoni for his technical help in the laboratory.

*Work coordinated with the Gruppo Nazionale Struttura della Materia program of the Italian National Research Council.

[1]B. M. Butcher, H. Hutto, and A. L. Ruoff, Appl. Phys. Letters 7, 34 (1965).

[2]H. R. Curtin, D. L. Decker, and H. B. Vanfleet, Phys. Rev. 139, A1552 (1965).

[3]A. Ascoli, B. Bollani, G. Guarini, and D. Kustudic, Phys. Rev. 141, 732 (1966).

[4]A. Ascoli, in *Chemical and Mechanical Behavior of Inorganic Materials*, edited by A. V. Searcy, D. Ragone, and U. Colombo (Wiley-Interscience, New York, 1970), p. 205.

[5]J. N. Mundy, Phys. Rev. B 3, 2431 (1971).

[6]S. J. Rothman, N. L. Peterson, and J. T. Robinson, Phys. Status Solidi 39, 635 (1970).

[7]W. Seith and A. Keil, Z. Physik. Chem. (Frankfurt) B22, 350 (1933); C. Wagner, *ibid.* B38, 325 (1938).

[8]A. S. Nowick, J. Appl. Phys. 22, 1182 (1951); Comments Solid State Phys. 1, 140 (1968).

[9]B. F. Dyson, T. R. Anthony, and D. Turnbull, J. Appl. Phys. 37, 2370 (1966).

[10]T. R. Anthony, B. F. Dyson, and D. Turnbull, J. Appl. Phys. 37, 2925 (1966).

[11]T. R. Anthony and D. Turnbull, Appl. Phys. Letters 8, 120 (1966).

[12]F. Van der Maesen and J. A. Brenkman, J. Electrochem. Soc. 102, 229 (1955); B. I. Boltaks, Zh. Tekhn. Fiz. 26, 457 (1956) [Sov. Phys. Tech. Phys. 1, 443 (1956)]; F. C. Frank and D. Turnbull, Phys. Rev. 104, 617 (1956); K. Weiser, *ibid.* 126, 1427 (1962).

[13]G. V. Kidson, Phil. Mag. 13, 247 (1966).

[14]B. F. Dyson, J. Appl. Phys. 37, 2375 (1966).

[15]T. R. Anthony and D. Turnbull, Phys. Rev. 151, 495 (1966).

[16]B. F. Dyson, T. R. Anthony, and D. Turnbull, J. Appl. Phys. 38, 3408 (1967).

[17]T. R. Anthony, B. F. Dyson, and D. Turnbull, J. Appl. Phys. 39, 1391 (1968).

[18]M. P. Dariel, G. Erez, and G. Schmidt, J. Appl. Phys. 40, 2746 (1969).

[19]G. M. Hood, in *Diffusion Processes*, edited by J. N. Sherwood, A. W. Chadwick, W. M. Muir, and F. L. Swinton (Gordon and Breach, New York, 1971), Vol. I, p. 361.

[20]J. W. Miller, in Ref. 19, p. 203.

[21]C. T. Candland, D. L. Decker, and H. B. Vanfleet, Phys. Rev. B 5, 2085 (1972).

PHYSICAL REVIEW B VOLUME 6, NUMBER 10 15 NOVEMBER 1972

Low-Energy-Electron Diffraction from Several Surfaces of Aluminum

D. W. Jepsen and P. M. Marcus
IBM Thomas J. Watson Research Center, Yorktown Heights, New York 10598

and

F. Jona*
Department of Materials Science, State University of New York, Stony Brook, New York 11790

(Received 9 May 1972)

A model for aluminum used previously for low-energy-electron-diffraction (LEED) calculations by the layer Korringa–Kohn–Rostoker method on the {001} surfaces, is carefully defined and used to find LEED spectra for the {111} and {110} surfaces. Agreement between theory and experiment is as good for {111} as for {001}, but is not as good for {110}, which appears generally to be a "bad actor." Close comparison of the shapes of lines in the experimental and theoretical spectra suggests values for the interlayer spacing of the outermost layer of the crystal which are roughly 5% greater than bulk for the {111} face but 10% less than bulk for the {110} face.

I. INTRODUCTION

A model for aluminum and method of calculation for low-energy-electron diffraction (LEED) has been described by us previously[1,2] with detailed application to Al{001}. This work gave satisfactory agreement with experimental LEED spectra (i.e., flux density in diffracted beams versus energy at fixed angles of incidence) on the {001} surfaces for energies up to 150 eV for several beams and for a range of incident polar angles (i.e., angles with the surface normal) from 0° to 25°. In the present paper, we apply the same model and calculation procedure to the {111} and {110} surfaces of Al and compare the results for all surfaces. We also take the opportunity to describe the model care-

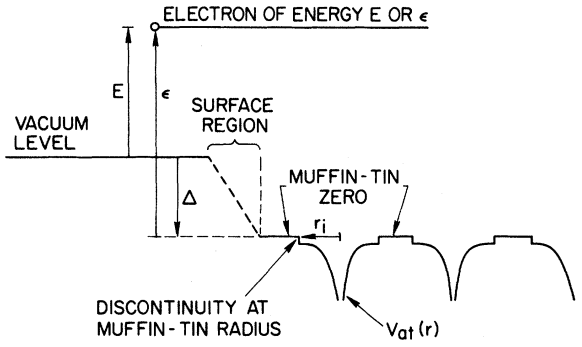

FIG. 1. Schematic picture of the model of the potential used for LEED calculations. Potential is plotted on a line normal to the surface and through the centers of a row of atoms. The level difference Δ, the discontinuity at the muffin-tin radius r_i, the atomic part of the potential $V_{at}(r)$, and the energy scales E and ϵ are shown.

fully, since it is not the same as others have used[3–5] for Al, and it is easy to be confused about some features. Finally, the model is further refined to include some specific surface effects by exhibiting the systematic changes in the LEED spectra produced by expansion or compression of the interlayer distance of the first atomic layer. These calculations show that groups of lines are sensitive to the change of spacing, and hence that some estimates of the outermost interlayer spacing are possible by comparison with experiment.

The method of calculation is conveniently called the layer Korringa–Kohn–Rostoker (KKR) method, since it consists in first treating the multiple scattering within a single layer of atoms by the KKR method of band theory[2,6,7] (extended to complex potentials) and in then treating the multiple scattering between layers by matrix methods based on a beam representation of the wave field (i.e., an expansion in plane waves all of which have the same energy and the same reduced component of wave number parallel to the surface[8]). The calculations use up to 29 beams and 8 phase shifts to achieve an accuracy in the calculated spectra of better than 2% at energies up to 150 eV. A correction for lattice motion is included which averages the scattering over the positions of an individual atom, assuming those positions form the spherical Gaussian distribution given by a Debye phonon spectrum ($\Theta_D = 418$ °K). The calculations also treat the matching conditions at the surface between interior and exterior wave fields in a way that allows for the change in potential level between vacuum and the interior of the specimen (plane waves are refracted), but so as to avoid the strong reflection of a sudden step in the potential (reflections from the surface region are completely suppressed; see discussion in Sec. II and Ref. 2).

II. MODEL FOR Al

The basis for the model is the Hartree–Fock–Slater self-consistent muffin-tin potential for Al calculated by Snow[9] to produce a band structure in reasonable agreement with Fermi-surface measurements.[10] This potential is supplemented by an imaginary part $-i\beta$ to describe inelastic (or incoherent) scattering of the electrons (i.e., such scattering is treated as equivalent to removal of the electron by absorption) and by specifying the vacuum level. In general, β is a function of both $\vec{r}$ and the electron energy. Since there is no adequate theory for β in a periodic solid, β has been taken independent of $\vec{r}$. Some idea of the energy dependence of β is given by the behavior of the imaginary part of the self-energy of an electron in a uniform (interacting) electron gas (i.e., interacting electrons moving in a smeared-out rigid positive charge),[11] which at the Al density ($r_s = 2.07a_0$, where r_s is the equivalent sphere radius and a_0 is the Bohr radius) is nearly constant between 30 and 150 eV with a value of about 0.3 Ry = 4.1 eV. We have adopted this value for β throughout the solid (including the insides of the muffin-tin spheres). However, the scattering by the atoms is calculated with the real potential given by Snow, including the discontinuity of 0.053 Ry (= 0.72 eV) at the muffin-tin radius r_i ($r_i = 2.7057a_0$ for Al) between the atomic potential $V_{at}(r)$ and the constant (higher) level between the atomic spheres; this constant level is referred to as the muffin-tin zero (see Fig. 1). The phase shifts $\eta_l(\epsilon)$ determining the asymptotic wave function are found from $V_{at}(r)$ (where ϵ is the energy with respect to the muffin-tin zero—*not* vacuum), and the scattering is treated as if point scatterers with these phase-shift functions were embedded in a uniform absorbing medium[12] of potential $-i\beta$.

Note that the band structure of Al is completely defined with respect to the muffin-tin zero by the above specification of the potential, although no mention has yet been made of the position of the vacuum level or the value of Δ, which gives the position of the muffin-tin zero with respect to the vacuum level. Thus the Fermi level is 8.2 eV above the muffin-tin zero, and the bottom of the conduction band is 2.8 eV below; the band structure computed for the above potential (with $\beta = 0$) agrees closely with that computed by Connolly[13] up to $\epsilon = 50$ eV also using the Snow potential.

The specification of the model is now completed by the value of Δ. In general, Δ is a function of E (the energy of the electron with respect to the vacuum level, $E = \epsilon - \Delta$). At $E = 0$ the magnitude of Δ (Δ is negative) would be 12.4 eV on adding the work function of 4.2 eV to the energy of the Fermi level above the muffin-tin zero. At higher

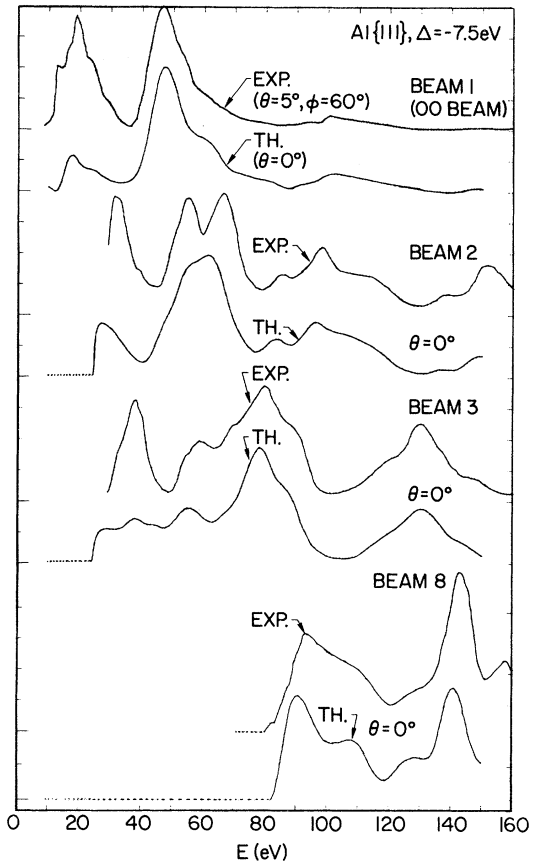

FIG. 2. Experimental (upper curves in each pair) and theoretical (lower curves) LEED spectra for Al{111} on a common energy scale E up to 160 eV. All spectra are at normal incidence except the 00 experimental spectrum, which is at $\theta = 5°$, $\phi = 60°$. The theoretical spectra are all computed with $\Delta = -7.5$ eV, $\beta = 4.1$ eV, the Snow potential and a correction for lattice motion at $T = 298$ °K and $\Theta_D = 418$ °K. The beams are labeled and angles defined as in Fig. 3(a). The ordinate scales are arbitrarily adjusted so that the largest peaks in each spectrum are about the same height.

E, the magnitude of Δ is expected to decrease, as indicated by the results for a uniform electron gas.[11] These results show a rise of 5 eV in the real part of the self-energy, most of it for E less than 30 eV, thus indicating that there is a part of the (negative) exchange-correlation energy which increases with energy, and reflecting the physical fact that correlation effects are smaller at higher E. In the absence of precise estimates of $\Delta(E)$, we have chosen a constant Δ to give a reasonable average fit between experimental and theoretical peak positions, and looked for variation in the fit to indicate the variation of Δ with E, which need not be the same in the periodic solid as in a uniform gas. A best Δ has been found for each surface, although, if the model is reasonable, the differences between surfaces should be small, amounting only to the contact potential differences.

Finally, we note that the model does not require specification of the exact behavior of the potential between interior and vacuum, as is schematically indicated by the dashed line in the surface region in Fig. 1. Instead of specifying the potential in that surface or transition region, we make the approximation that plane waves, i.e., beams, that have enough energy in the normal direction to propagate in vacuum will cross the transition region from either the vacuum or the crystal side without reflection (but with proper change of energy from E to ϵ or ϵ to E and proper refraction). Thus we neglect the finite, but generally small, reflection produced by the actual potential, which has a smooth variation in the transition region. An assumption must also be made about the beams in the crystal with insufficient normal energy to propagate in vacuum. Usually we assume such beams are completely absorbed in the surface region, corresponding to the effects of surface plasmons and other excitations in that region, and we neglect any reflection of such beams. Thus the surface boundary conditions on both kinds of beams (propagating or nonpropagating in vacuum) may be succinctly specified as a "no-reflection" boundary condition. However, we have also calculated LEED spectra with the opposite boundary condition for nonpropagating beams, namely, total reflection from the surface region. In all cases studied there was no significant change in the spectrum. Thus we feel that the "no-reflection" model gives reliable LEED spectra with the desirable features of simplicity and universality but at the cost of omitting special phenomena which depend sharply on the detailed surface-region behavior (e.g., surface-resonance phenomena[14]).

III. COMPARISON OF EXPERIMENTAL AND THEORETICAL SPECTRA FOR THE {111} SURFACES

Experimental and theoretical LEED spectra computed with the above model of Al for {111} surfaces are plotted in Fig. 2 on a common energy scale out to 150 eV for four beams and for the case of normal incidence—except for the experimental specularly reflected (00) beam, which is at $\theta = 5°$, $\phi = 60°$ (the angle θ is with the normal; ϕ is defined in Fig. 3, which also gives the beam labeling). Note that for $\theta = 0°$, the set of beams numbered 2, 4, and 6 are degenerate, as are beams 3, 5, and 7, but the two sets are distinct, since the crystal has threefold, but not sixfold symmetry[15] around ⟨111⟩. However, beams 8–13 are sixfold degenerate, because of the presence of mirror planes. With the standard values $\Delta = -7.5$ eV and $\beta = 0.3$ Ry (4.1 eV) used previously for the {001} spectra, all corresponding experimental and theoretical spectra

are in comparably good agreement to the {001} results. We note that there is a peak at 60 eV in beam 2 which is split experimentally but not theoretically, and the theoretical peaks below 40 eV are relatively too small (which could be due to use of a constant β below 40 eV where β probably decreases), but, in general, peak positions, widths, and shapes agree very well. The same degree of agreement is shown in the spectra at $\theta = 5°$, $\phi = 60°$ in Fig. 4, although now beams 4 (or 2) and 6 are very different—as are beams 7 (or 5) and 3. Finally, in Fig. 5, we show that the same satisfactory agreement for the {111} surface appears at $\theta = 15°$, $\phi = 60°$. A detailed comparison of the positions of all peaks up to 150 eV in the {111} experimental and theoretical spectra gives an average value of Δ and mean-square deviation from that value of -6.5 ± 2.2 eV, to be compared with $\Delta = -7.8 \pm 1.6$ eV for the {001} surfaces.[16] Thus the agreement is about equally good on these two surfaces, and they show nearly equal values of the magnitude of Δ which are both substantially smaller than the values estimated from the work function (and the Fermi energy).

The degree of agreement between theory and ex-

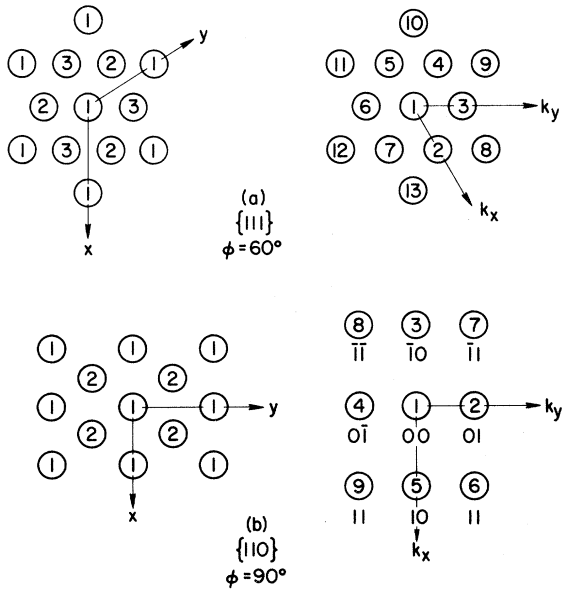

FIG. 3. Space lattices (left) and reciprocal lattices (right) for two surfaces of a fcc crystal. The plane of incidence is horizontal (perpendicular to the page and from left to right). The reciprocal lattice then shows the pattern of beam spots on the viewing screen. (a) The {111} surface for $\phi = 60°$: the first three atomic layers of the space lattice are labeled; the beams in the reciprocal lattice are sequence numbered. (b) The {110} surface for $\phi = 90°$: two atomic layers are labeled; three shells of beams are sequence numbered and labeled by the usual reciprocal-lattice-vector indices.

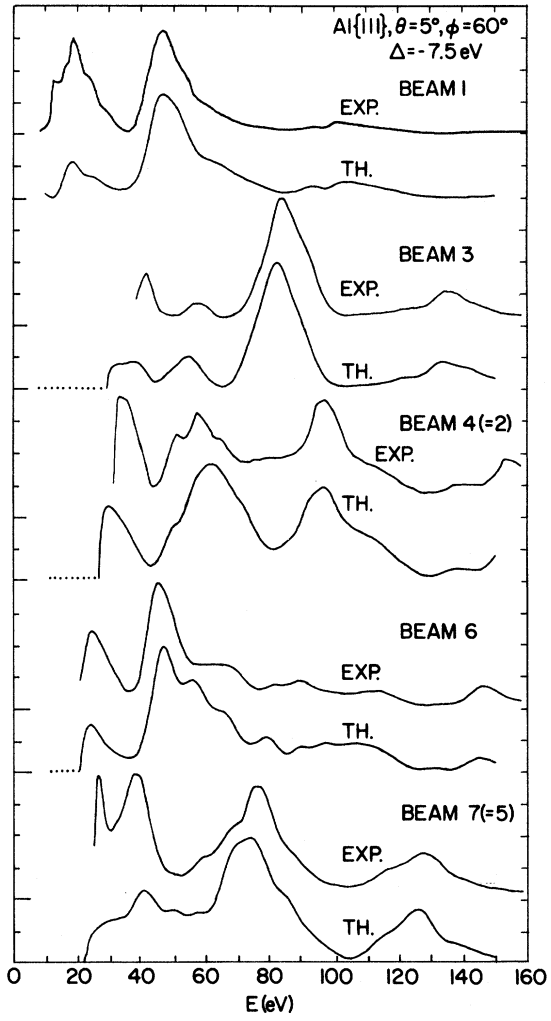

FIG. 4. LEED spectra for Al{111}, as in Fig. 2 except all spectra are at $\theta = 5°$, $\phi = 60°$.

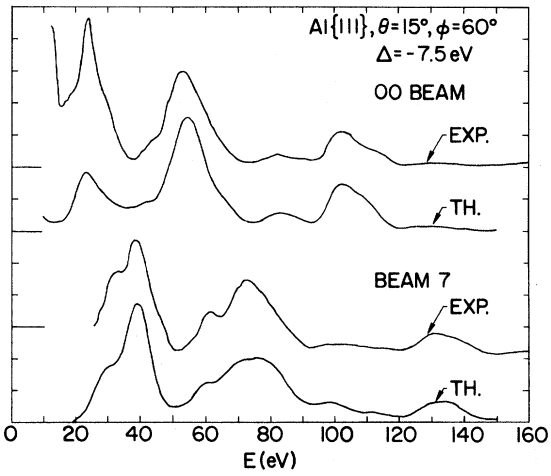

FIG. 5. LEED spectra for Al{111}, as in Fig. 2 except all spectra are at $\theta = 15°$, $\phi = 60°$.

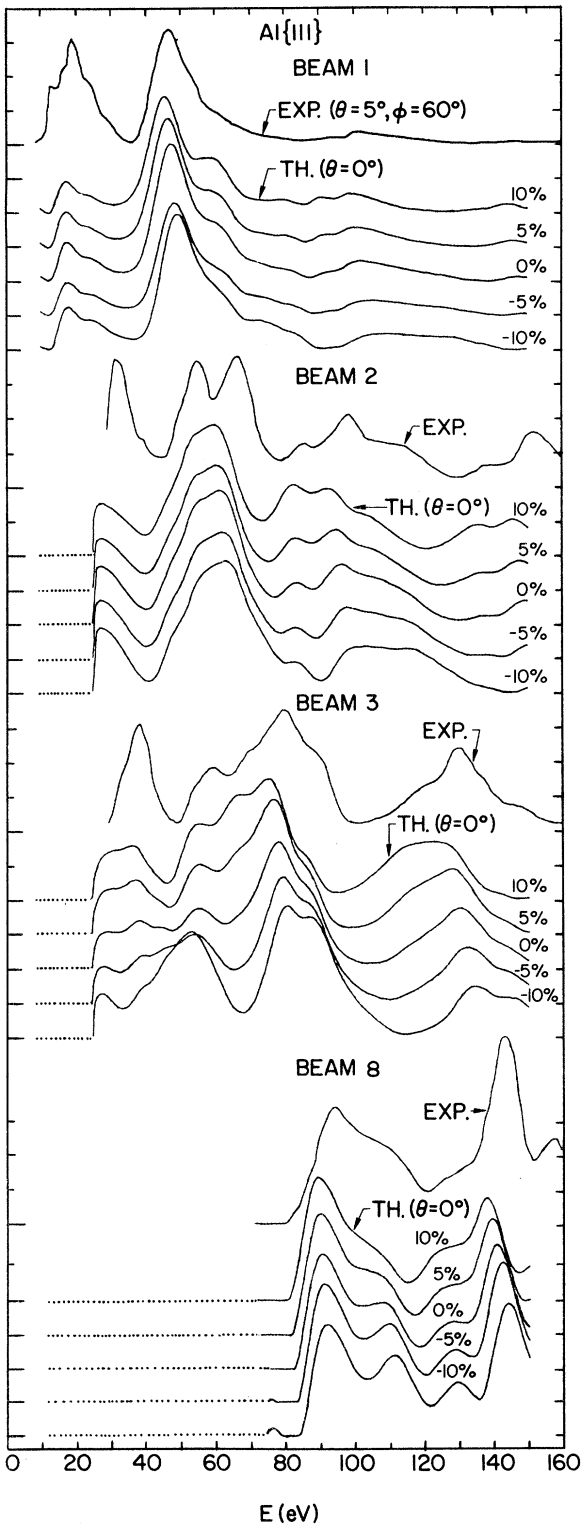

FIG. 6. LEED spectra for Al{111} as in Fig. 2 (with the same beams and angles) plus additional theoretical spectra for lattices with spacing of outermost atomic layer from substrate changed by 10, 5, −5, and −10% with respect to the bulk spacing.

periment achieved with this model leads us to attempt to draw a more refined conclusion from the experimental spectra—namely, by varying the spacing of the outermost layer from the second layer by up to ±10% of the bulk spacing, we look for indications of expansion or contraction of the lattice at the surface. A set of theoretical spectra obtained in this way is shown in Fig. 6, where the bulk layer spacing ($a\sqrt{3}/3$, where a is the side of the cubic unit cell) is used in calculating the middle curve. By examining the shapes of various groups of peaks and peak-shoulder combinations which are sensitive to the interlayer spacing, examples of which can readily be found in the sets of curves in Fig. 6, we see some evidence for an expansion of the {111} face. This comparison of shapes seems preferable to using peak positions to indicate change in interlayer spacing, which is difficult for the rounded peaks which occur here, especially when the shapes are different. Thus in beam 2 the observed pronounced peak at 95 eV is made more prominent in the theoretical spectra by an expansion, whereas a contraction tends to bury it; similarly the peak observed at 140 eV is brought out better in the calculated spectra by expansion, whereas contraction suppresses it. Elsewhere (for example, the peak at 85 eV and the shoulder at 115 eV) the evidence for expansion is less clear, and the observed but unexplained double peak around 60 eV prevents our drawing any conclusion about spacing. In beam 3 the calculated peaks at 35 and 70 eV and their relation to the background are brought closer to the experiment by expansion than contraction, as is true of the shoulders at 90 and 110 eV. Finally in beam 8 the shapes of the group of peaks between 90 and 120 eV and between 120 and 140 eV seem definitely closer to experiment by expansion than by contraction. (Note that the specular beam, beam 1, cannot be used in this analysis because the experimental spectrum is not available at normal incidence.) The over-all indication of somewhere around 5% expansion is the same as a similar analysis of the results on the {001} surfaces.[17] However, we shall show below that {110} is very different.

IV. COMPARISON OF THEORY AND EXPERIMENT FOR THE {110} SURFACES

Applying the same model and computational procedure to the {110} surfaces for a sequence of surface layer spacings, leads to the results plotted in Fig. 7 for $\theta = 5°$ and $\phi = 90°$ [angles and beams defined in Fig. 3]. The theoretical curves are all plotted at the Δ of -7.5 eV which gives good correspondence for the other two faces but which appears to be too large for this face. Comparing the bulk spacing curve (labeled 0%) with the experi-

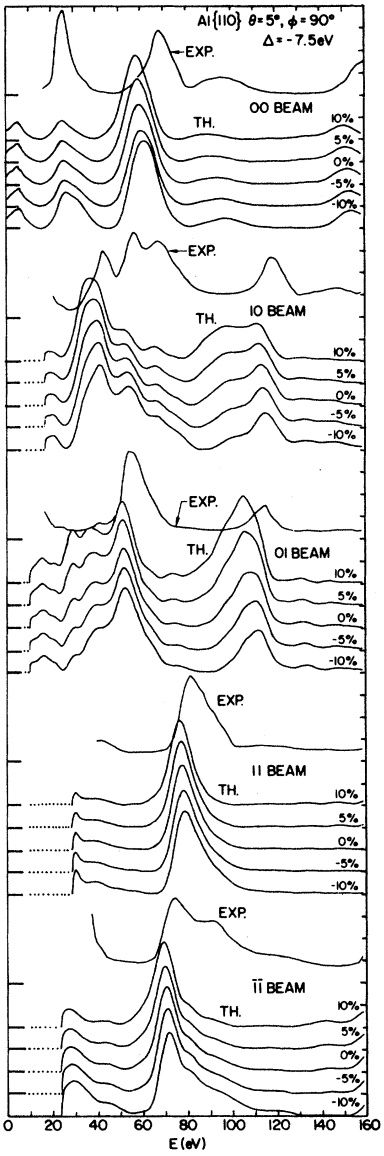

FIG. 7. Experimental and theoretical LEED spectra for Al{110} on a common energy scale E up to 160 eV at $\theta = 5°$, $\phi = 90°$ [angle definitions and beam labeling as in Fig. 3(b)]. Theoretical spectra are computed as for Fig. 2, and the same sequence of outermost atomic layer spacings is shown as in Fig. 6.

mental curve, we find that a value for Δ of -4.1 ± 2.1 eV gives best agreement. The agreement is still not as good as that found for the other two faces, and in particular, there are two peaks, at 70 and 160 eV, for which the correspondence is worse than for others.

We observe in Fig. 7 that the shapes of a number of the peaks and shoulders correspond slightly better with experiment in the curves for 10% contraction (labeled −10%) than in other curves in the figure. As evidence for this tentative conclusion, we note the partial suppression of the shoulder in the 10 beam at 100 eV, the change in shape of the peak at about 110 eV in the 01 beam, and the development of the shoulder at 80 eV in the $\bar{1}\bar{1}$ beam.

An additional effect of the contraction is to move all the computed peaks systematically to higher energies. Thus, the shift Δ of the theoretical spectrum of a contracted surface giving the best fit with experiment is nearer to the value used on the other faces (-7.5 eV) than is the Δ of the uncontracted surface. Figure 8 shows the experimental curves plotted with theoretical curves calculated for 10% contraction and shifted by a Δ of -5.0 eV (the best value of Δ from Fig. 8 is -5.3 ± 2.5 eV). This effect of contraction has been pointed out by Laramore and Duke,[5] who also con-

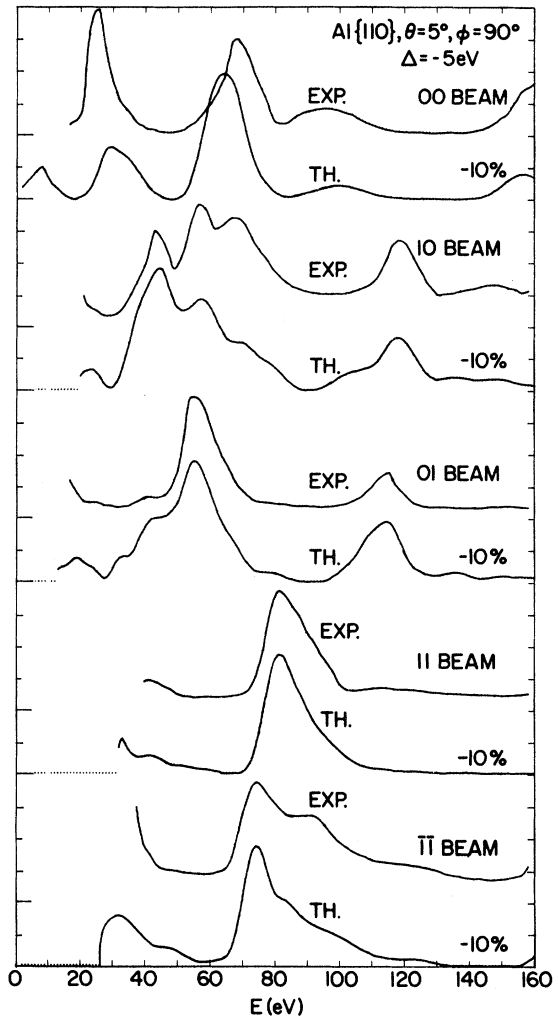

FIG. 8. LEED spectra for Al{110} as in Fig. 7 except with $\Delta = -5.0$ eV and only the theoretical spectra for a 10% contraction of the outermost layer spacing compared to bulk are shown.

clude that 10% contraction of the outer-layer spacing gives better agreement for the {110} faces.

The generally poorer agreement with experiment that this model of Al gives for the {110} faces, the somewhat different Δ, and the remarkable contraction suggested both by change of shape and movement of positions of peaks all combine to characterize the {110} face of Al as a "bad actor" among the faces.[18] Some additional evidence for this conclusion comes from certain features of the experiment. Thus the {110} surfaces were more difficult to prepare with acceptably smooth and mirrorlike surface finish than either {001} or {111}. The LEED patterns from {110} are in general not as good as from {111} and {001}: The background is slightly higher, the diffraction spots slightly broader, the contrast is worse. With varying electron energy, the diffraction spots pass through alternating sharp and slightly diffuse (as though defocussed) stages.[19] Whatever interpretation is given of these phenomena, it is likely to involve morphological irregularities of the Al{110} surface as prepared, e.g., a distribution of mono- and multiatomic steps. Previous studies[20] have in fact revealed that Al{110} shows a pronounced tendencey toward the development of {111} facets.

---

*Research supported in part by the Air Force Office of Scientific Research (AFSC) under Grant No. AFOSR-72-2151.

[1]D. W. Jepsen, P. M. Marcus, and F. Jona, Phys. Rev. Letters 26, 1365 (1971).

[2]D. W. Jepsen, P. M. Marcus, and F. Jona, Phys. Rev. B 5, 3933 (1972).

[3]S. Y. Tong and T. M. Rhodin, Phys. Rev. Letters 26, 711 (1971).

[4]G. E. Laramore, C. B. Duke, A. Bagchi, and A. B. Kunz, Phys. Rev. B 4, 2058 (1971).

[5]G. E. Laramore and C. B. Duke, Phys. Rev. B 5, 267 (1972).

[6]D. W. Jepsen and P. M. Marcus, *Computational Methods in Band Theory* (Plenum, New York, 1971), p. 416.

[7]E. Kambe, Z. Naturforsch. 22a, 322 (1967); 22a, 422 (1967).

[8]P. M. Marcus and D. W. Jepsen, Phys. Rev. Letters 20, 925 (1968). Such a representation is a natural one in vacuum where the amplitudes of the plane waves remain constant. It is also convenient to use in a solid with a given periodicity in the xy plane (parallel to the surface), in which case the plane-wave amplitudes become functions of z.

[9]E. C. Snow, Phys. Rev. 158, 683 (1967), see Table I. The potential used for the phase-shift calculations $\eta_l(\epsilon)$ added 0.831 Ry to each entry in Table I.

[10]J. S. Faulkner, Phys. Rev. 178, 914 (1969).

[11]B. Lundqvist, Phys. Status Solidi 32, 273 (1969).

[12]This procedure avoids the necessity of computing complex phase shifts which would be produced if $-i\beta$ were added to $V_{at}(r)$ inside the muffin-tin spheres.

[13]J. W. D. Connolly, Intern. J. Quant. Chem. IIIS, 807 (1970). Our band structure is shown in detail in Ref. 2.

[14]See, for example, E. G. McRae, Surface Sci. 25, 491 (1971).

[15]From the hexagonal arrangement of the atoms in the top layer of the crystal, one might expect the LEED pattern to have sixfold symmetry. However, the lateral displacement of the layer below the top layer reduces the symmetry to threefold even though the 00 reflection still shows sixfold symmetry [M. G. Lagally, T. C. Ngoc, M. B. Webb, Surface Sci. 2, 444 (1971)]. The direction of this displacement was not determined in orienting the crystal before measurement, but crude comparison of the nonspecular beam results quickly resolves this ambiguity.

[16]In their work, Laramore and Duke (Ref. 5) draw no conclusion about the outer-layer spacing for the {100} and {111} surfaces, and find rather poorer agreement between theory and experiment for the {111} face compared to the {100}. With a Δ (their $-V_0$) of -16.7 eV for the {110} face, their calculated peaks are consistently lower than the experimental peaks by 10 to 15 eV. These differences from our results appear to be a consequence of the different potential they use for Al. Although they also start from Snow's (Ref. 9) paper on Al, they calculate rather different phase shifts by using -1.225 Ry for the muffin-tin zero, but -0.883 Ry (from Snow's Table I) for the atomic potential at the muffin-tin radius—hence a discontinuity of -0.342 Ry compared to our $+0.053$ Ry. We regard this potential as a misinterpretation of Snow's potential, and confirm our potential by the correspondence in our band structures with Connolly's and Snow's band structures.

[17]P. M. Marcus, D. W. Jepsen, and F. Jona, Surface Sci. 31, 180 (1972).

[18]Laramore and Duke also conclude from their analysis that {110} is a bad actor. However, they conclude that an additional shift of 10–15 eV is needed to fit theory and experiment compared to the {100} and {111} surfaces, i.e., that $\Delta_{110}-\Delta_{001}=10$ to 15 eV. Our Δ values for the different surfaces correspond much more closely—thus $\Delta_{110}-\Delta_{001}=-7.8+4.1=3.7$ eV. These differences may well be due to the different potential they use, as described in Ref. 16.

[19]A possible interpretation of this observation is that Al{110} surfaces, as prepared by us, contain a certain number of very small high-index surfaces, a phenomenon that may be called microfaceting. These microfacets would be too small to produce visible "maverick beams," as Lander [in *Progress in Solid State Chemistry*, edited by H. Reiss (Pergamon, Oxford, 1965), Vol. 2, p. 51] called them, but large enough to contribute the general impression of diffuseness when electrons are diffracted by them in the regions of reciprocal space centered around the intense beams from the main surface.

[20]F. Jona, J. Phys. Chem. Solids 28, 2155 (1967); S. M. Bedair and H. P. Smith, Jr., Appl. Phys. 42, 3616 (1971).